

Theoretical Analysis of Film Thickness Transition Dynamics and Coalescence of Charged Miniemulsion Droplets

Dimiter N. Petsev

Center for Microgravity and Materials Research, University of Alabama in Huntsville,
Huntsville, Alabama 35899

Received August 27, 1999. In Final Form: October 28, 1999

The kinetics of thickness transitions of the film, separating two electrostatically stabilized emulsion droplets, is studied. The film evolution is considered as a random process in the two-dimensional space of the film radius and thickness. The analysis is based on the Smoluchowski equation for the time dependent probability for realization of a given configuration (film radius and thickness). The combination of attractive and repulsive (van der Waals and electrostatic) energies determines the potential energy term in the Smoluchowski equation, while the hydrodynamic resistance of film thinning determines the diffusion tensor. The components of the latter are calculated. This approach allows one to obtain the average escape time from the secondary (common film) to the primary (Newton black film) energy minimum. This is equivalent to the common film lifetime. If there are not any short-ranged repulsions, to stabilize the thin (Newton black) film, the droplets fuse and the average escape time becomes that for coalescence. It is shown that the droplet deformability may have a great impact on the kinetics of film thickness transition. This is particularly important for emulsion systems with low interfacial tension and high electrolyte concentrations.

I. Introduction

Film formation and thinning upon approach and interaction of two droplets are among the crucial factors determining emulsion stability.^{1,2} They present also an important difference between flocculation of fluid particles and solid ones where no deformation takes place. The kinetics of aggregation of solid particles was treated in the beginning of the century by Smoluchowski.³ The same approach was recently modified to account for the droplet deformability and film formation.⁴ There, the Smoluchowski idea³ for calculating the coagulation rate from the steady flux of one particle toward the other was combined with effects of the droplet deformability and film formation. The film formation was considered to be due to the balance of the force driving the droplets together and the hydrodynamic resistance of the fluid captured in the gap. It was shown that the deformability has virtually no impact on the coalescence dynamics of micron-sized droplets if only attractive (e.g., van der Waals) forces are present. This is not the case, however, if there is a superposition of attractive and repulsive interactions, like in the typical Derjaguin–Landau–Verwey–Overbeek (DLVO) model.^{5,6} Two droplets may flocculate and deform, with a planar film separating their surfaces, in the secondary (more distant) minimum^{7–9} see (Figure 1a).

Depending on the magnitudes of the energy contributions such a doublet has the following options:² (i) The film jumps into the primary (closer) minimum, decreasing its thickness and increasing its radius. The stability of the doublet in the primary minimum requires short range repulsion of non-DLVO origin. (ii) The film breaks and the droplets coalesce, if no short range repulsion is present. (iii) The droplets separate.

If the repulsive forces are not very strong or long-ranged, the attraction dominates^{7–9} and the last option is least likely. The kinetics of transition into the primary minimum (or coalescence, if the latter is not stable) depends on the mean escape time from the secondary potential well (see Figure 1a). For certain interaction energies and droplet volume fractions, this escape time could be much greater than the one necessary for the droplets to approach, and thus it would determine the overall transition and/or coalescence dynamics. In other words, the transition over the energy barrier between the secondary and primary minima could be the rate-determining stage. This is the case we are focusing on in the present study. It is, in some aspects, complementary to ref 4 by defining appropriate boundary conditions at the droplet contact. The present consideration refers to the case where the droplets have already collided and formed a (relatively) stable doublet with a film between them due to the balance of the attractive and repulsive surface forces. Since we will restrict ourselves to the DLVO case, these are van der Waals and electrostatic forces.^{5,6} The kinetics of arrival into the secondary (more distant) minimum could be described in terms of the previous model,⁴ but in this study we are interested only in the transition from the secondary into the primary minimum, across the energy barrier.

An approach for direct experimental observation of foam and emulsion films is to mimic them in specially designed cell.^{10,11} This experimental cell, however, is relevant for films formed between millimeter-sized drops (or bubbles).

(1) Dukhin, S. S.; Rulev, N. N.; Dimitrov, D. S. *Coagulation and Dynamics of Thin Films*; N. Dumka: Kiev, 1980 (in Russian).

(2) Ivanov, I. B.; Kralchevsky, P. A. *Colloids Surf.* **1996**, *128*, 151.

(3) von Smoluchowski, M. *Phys. Z.* **1916**, *17*, 557; *Phys. Z.* **1916**, *17*, 785; *Z. Phys. Chem.* **1917**, *92*, 129.

(4) Danov, K. D.; Denkov, N. D.; Petsev, D. N.; Ivanov, I. B.; Borwankar, R. *Langmuir* **1993**, *9*, 1731.

(5) Derjaguin, B. V. *Theory of Stability of Colloids and Thin Films*; Plenum: New York, 1989.

(6) Verwey, E. J. W.; Overbeek, J. Th. G. *Theory of the Stability of Lyophobic Colloids*; Elsevier: Amsterdam, 1948.

(7) Denkov, N. D.; Petsev, D. N.; Danov, K. D. *Phys. Rev. Lett.* **1993**, *71*, 3226.

(8) Petsev, D. N.; Denkov, N. D.; Kralchevsky, P. A. *J. Colloid Interface Sci.* **1995**, *176*, 201.

(9) Petsev, D. N. In *Modern Aspects of Emulsion Science*; Binks, B. P., Ed.; Royal Society of Chemistry: London, 1998; Chapter 10.

(10) Scheludko, A. *Adv. Colloid Interface Sci.* **1967**, *1*, 391.

(11) Scheludko, A.; Exerowa, D. *Kolloid Z.* **1957**, *155*, 37.

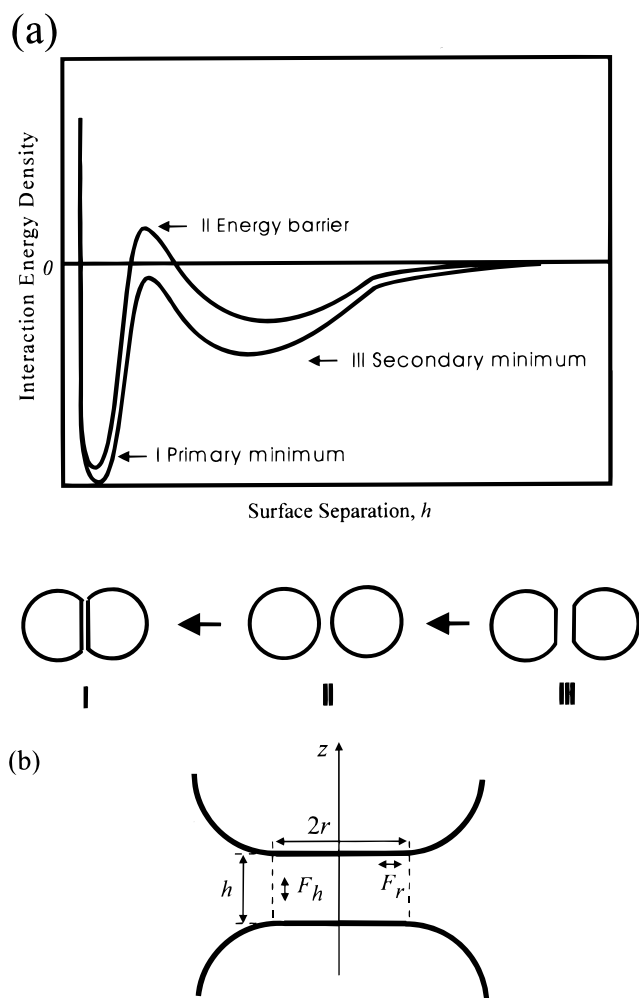


Figure 1. A schematic representation of (a) the interaction energy density per unit area profile for deformable emulsion droplets. Depending on the parameters, the barrier could be higher or lower than the referent zero energy (at infinite separation); (b) planar film between the droplets, its parameters, and radial and normal forces (see the text). z is the axis of cylindrical symmetry.

Recently a redesigned version was suggested¹² that is considerably miniaturized and allows the range of films about hundreds of micrometers to be covered. It was shown¹² that there are significant differences in the film behavior, depending on its size. Thus the thinning kinetics is much faster for small films, compared to large ones, and the film surfaces seem to lack corrugations and dimple formation. The films we are interested in the present study occur between Brownian droplets and therefore are smaller even than those studied in ref 12. Such small films have not been subject to direct experimental study yet. Hence, it is our belief that a theoretical estimate of the thinning and thickness transition kinetics in mini-emulsions is important to understand and further model the behavior of the macroscopic emulsion system consisting of submicrometer droplets (mini-emulsion).

An extensive study of the flocculation kinetics and doublet stability of emulsion droplets was performed recently by Holt et al.,^{13,14} using video-enhanced microscopy. The measured lifetimes of the doublets range from

minutes to tens of hours. All these neglect the possible contribution of the deformability of the doublets. This is justified for the salt concentrations considered, which are low compared to those relevant to the present study. As we show below, there are still many cases where the deformability may have an impact on the flocculation kinetics and doublet stability. However, a quantitative comparison between our results and those in refs 13 and 14 is not possible because, as mentioned above, we are interested in smaller droplets and higher electrolyte concentrations. The calculations, presented below, are for model systems with a reasonable set of parameters, often encountered in emulsions. Good examples are oil/water/surfactant/salt systems, which are known to exhibit very low interfacial tension values at certain ionic strengths.^{15,16}

The paper is organized as follows: in the next section the formulation of the model is discussed, section III deals with derivation of the time of escape from the secondary minimum, section IV presents the expressions for the equilibrium distribution function and diffusion tensor, section V presents some numerical results for droplets with tangentially immobile surfaces, and section VI summarizes the conclusions. The calculation of the diffusion tensor components is given in the Appendix.

II. Problem Formulation and Basic Assumptions

The central point in our consideration is based on the notion that once the film is formed, its parameters (radius, r , and thickness, h) fluctuate around the equilibrium state, due to the thermal energy of the system. Therefore, the realization of different combinations of r and h at different moments, t , is a random process taking place with time in the two-dimensional space of the film radius and thickness. It is convenient to visualize it as a diffusion of a virtual Brownian particle in the r, h space. This particle is subject to the action of an external energy field and viscous drag, which are due to the thermodynamic and hydrodynamic interactions of the droplet's surfaces. The Smoluchowski problem,³ as well as its recent modification for deformability,⁴ is to account for the translational approach of two freely diffusing particles. It is effectively one-dimensional, because of the spherical symmetry. In the present case we consider a doublet of spheres in contact and the fluctuations of the radius and thickness of the planar film formed between them. Therefore, the stability problem is apparently two-dimensional since there is a cylindrical symmetry (see Figure 1b).

The main assumptions we introduce in the present model are the following:

- (1) The shape of the deformed droplets remains that of truncated spheres for all values of r and h .
- (2) The parameters of the interacting surfaces, like surface charge and interfacial tension, do not change with the film radius and thickness fluctuations. This means, for example, that there is no coupling between the hydrodynamic flows with ion fluxes toward the droplet surfaces that may change the electrostatic potential.
- (3) The expressions for the surface and hydrodynamic forces, which we use below, were derived under certain assumptions which are discussed in the relevant references.^{4,7-9,19-21,24-26}

(14) Holt, O.; Saether, O.; Sjoblom, J.; Dukhin, S. S.; Mischuk, N. A. *Colloids Surf. A* **1998**, *141*, 269.

(15) Aveyard, R.; Binks, B. P.; Mead, J. *J. Chem. Soc. Faraday. Trans. 1* **1985**, *81*, 2169.

(16) Aveyard, R.; Binks, B. P.; Clark, S.; Mead, J. *J. Chem. Soc. Faraday. Trans. 1* **1985**, *82*, 125.

(17) Gardiner, C. W. *Handbook of Stochastic Methods*, 2nd ed.; Springer: New York, 1986.

(12) Velev, O. D.; Constantinides, G. N.; Avraam, D. G.; Payatakes, A. C.; Borwankar, R. P. *J. Colloid Interface Sci.* **1995**, *175*, 68.

(13) Holt, O.; Saether, O.; Sjoblom, J.; Dukhin, S. S.; Mischuk, N. A. *Colloids Surf. A* **1997**, *123-124*, 195.

(4) The film radius and thickness fluctuations are assumed to be uncoupled to the translational and rotational diffusion modes of the doublet.

Since the interaction energy depends not only on the distance between the droplets (film thickness) but also on the extent of deformation (film radius), it is convenient to present its energy in terms of contour diagrams (see Figures 2 and 4) instead of plots like Figure 1a.

III. Probability Function and Escape Time

The radial and thickness fluctuations of the film between the droplets are considered as a Brownian motion of a virtual particle in the two-dimensional space of the film radius, r , and film thickness, h . The probability function, $P(r, h, t)$, for the realization of a given configuration (values of r and h) at time t obeys the Smoluchowski equation^{17,18}

$$\frac{\partial P(r, h, t)}{\partial t} = \nabla \cdot \{ \mathbf{D}(r, h) \cdot [\nabla P(r, h, t) + P(r, h, t) \nabla \beta U(r, h)] \} \quad (1)$$

where $\mathbf{D}(r, h)$ is the diffusion tensor, $U(r, h)$ is the energy field, $\beta = 1/kT$ is the inverse thermal energy, and ∇ is the differential operator in the r, h space. If we write the probability function as $P(r, h, t) = P_{\text{eq}}(r, h) \tilde{P}(r, h, t)$, eq 1 can be written in the adjoint form^{17,18}

$$\frac{\partial \tilde{P}(r, h, t)}{\partial t} = \frac{1}{P_{\text{eq}}(r, h)} \nabla \cdot [P_{\text{eq}}(r, h) \mathbf{D}(r, h) \cdot \nabla \tilde{P}(r, h, t)] \quad (2)$$

The equilibrium probability is

$$P_{\text{eq}}(r, h) = \exp[-\beta U(r, h)] \quad (3)$$

There is no need to normalize the equilibrium probability (see eq 3), because it always enters in such combinations that the normalization constant cancels (see below).

Let the initial state of the system be in close vicinity of the secondary minimum with respect to r and h . We consider a region bounded from below by $r = 0$ and $h = h^*$ (the latter corresponds to the h -coordinate of the saddle point in the energy surface. The upper value for r could be set to infinity, since the energies for $r/a \rightarrow 1$ are so high that such realizations are effectively excluded. Clearly the system (characterized by given values for r and h) cannot leave this region across $r = 0$, $r/a \rightarrow 1$, or $h = \infty$. The only option left is across the boundary $h = h^*$. The average escape time from this region is defined by $\tau(r, h) = \int_0^\infty dt \tilde{P}(r, h, t)$.^{17,18} Integrating eq 2 over time yields^{17,18}

$$\frac{1}{P_{\text{eq}}(r, h)} \nabla \cdot [P_{\text{eq}}(r, h) \mathbf{D}(r, h) \cdot \nabla \tau(r, h)] = -1 \quad (4)$$

(18) van Kampen, N. G. *Stochastic Processes in Physics and Chemistry*, 2nd ed.; Elsevier: New York, 1992.

(19) Danov, K. D.; Petsev, D. N.; Denkov, N. D.; Borwankar, R. *J. Chem. Phys.* **1993**, *99*, 7179; *J. Chem. Phys.* **1994**, *100*, 6104.

(20) Klahn, J. K.; Agterof, W. G. M.; van Voorst Vader, F.; Groot, R. D.; Graenweg, F. *Colloids Surf.* **1992**, *65*, 161.

(21) Hamaker, H. C. *Physica* **1937**, *4*, 1058.

(22) Onsager, L. *Phys. Rev.* **1931**, *37*, 405.

(23) Israelachvili, J. N. *Intermolecular and Surface Forces*, 2nd ed.; Academic Press: New York, 1995.

(24) Ivanov, I. B.; Dimitrov, D. S. In *Thin Liquid Films*; Ivanov, I. B., Ed.; Marcel Dekker: New York, 1988, Chapter 7.

(25) Traykov, T. T.; Ivanov, I. B. *Int. J. Multiphase Flow* **1977**, *3*, 471.

(26) Henderson, D.; Duh, D.-M.; Chu, X.; Wasan, D. T. *J. Colloid Interface Sci.* **1997**, *185*, 265.

This is an equation for the mean escape time $\tau(r, h)$ the system needs to leave the region defined above. The right hand side comes from the fact that the probability to find the system in the region is 1 at moment $t = 0$ (initial condition) and 0 at $t = \infty$ (given enough time the system will prefer the lower energy state, the primary minimum). For details of this argument see refs 17 and 18). Hence,

$$\int_0^\infty dt \frac{\partial \tilde{P}(r, h, t)}{\partial t} = \int_0^\infty d\tilde{P}(r, h, t) = \tilde{P}(r, h, \infty) - \tilde{P}(r, h, 0) = -1 \quad (5)$$

Equation 4 allows one to find the escape time or the lifetime of the thick (secondary) film between the emulsion droplets if $P_{\text{eq}}(r, h)$ and $\mathbf{D}(r, h)$ are known. The problem bears mathematical difficulties because it is two-dimensional and its general form, shown above, allows only for numerical solution or analytical estimations in some particularly simple cases.¹⁸ As we show below, however, for the case of immobile droplet surfaces, eq 4 reduces to one-dimensional form and therefore is amenable to significant simplifications without loss of accuracy. Emulsions with immobile droplet surfaces correspond to systems in which the surfactants are in high concentrations and are present in the continuous phase only. Such case is commonly encountered in practice.

IV. Equilibrium Probability $P_{\text{eq}}(r, h)$ and Diffusion Tensor $\mathbf{D}(r, h)$

A. Surface Forces. The equilibrium probability for realization of a given configuration, r, h , depends on the energy, $U(r, h)$. The particular form of this energy is in accordance with the specific type of colloidal forces acting between the surfaces. For emulsion droplets there is a wide variety of such energy contributions.^{8,9} Here, we restrict our consideration to the typical DLVO case where two major forces are operative: electrostatic repulsion and van der Waals attraction.^{5,6} Short-ranged non-DLVO repulsion accounts for the stability of the primary films. The introduction of any other type of surface forces, when considering deformable droplets, is straightforward.^{8,9}

Exact expression for the van der Waals attraction between truncated spheres has been recently derived by a number of authors,^{19,20} following the method of Hamaker.²¹ The general result for truncated spheres is rather lengthy,^{19,20} but fortunately most practically important cases allow for substantial simplifications without loss of accuracy.^{4,7-9,19} Thus for relatively small droplets deformations ($r^2/a^2 \ll 1$) we arrive at the following expression for the van der Waals attraction¹⁹

$$U_{\text{vw}}(r, h) = -\frac{A_H}{12} \left\{ \frac{4a^2}{(2a+h)^2} + \frac{4a^2}{h(4a+h)} + 2 \ln \left[\frac{h(4a+h)}{(2a+h)^2} + \frac{128a^5 r^2}{h^2(2a+h)^3(4a+h)^2} \right] \right\} \quad (6)$$

where A_H is the Hamaker constant. The first three terms in the right hand side are identical to the case of interacting undeformed spheres solved by Hamaker,²¹ while the last one appears due to the deformability of the fluid droplets and is proportional to r^2 .

The electrostatic repulsion between colloidal particles can be calculated analytically only if significant approximations are made. Often used is Derjaguin's ap-

proximation,⁵ which for truncated spheres gives^{4,7–9,19}

$$U_{\text{el}}(r, h) = \pi \epsilon_0 \epsilon \kappa \Psi_0^2 \left\{ \left[1 - \tanh\left(\frac{\kappa h}{2}\right) \right]^2 r^2 + \frac{2a}{\kappa} \ln[1 + \exp(-\kappa h)] \right\} \quad (7)$$

Equation 7 holds for moderately high (<25 mV) and constant surface potentials. Again, there is a term that is equivalent to undeformed sphere interaction (the second in the right hand side) and another one, which proportional to the film area. Other alternative expressions for the electrostatic energy, depending on the particular situation and relevant approximations are available as well.^{5,6,19}

In order to have a stable configuration into the primary minimum, a short-ranged repulsive force is needed. Otherwise the thin primary film will not be stable. A possible candidate is the hydration repulsive interactions.²³ A source of repulsion could be also derived by integrating the short-ranged term in the Lennard–Jones potential, as in ref 26. This approach gives a very convenient simple power expression for the short-ranged repulsion, U_{sr} , which can be simply utilized in the consideration of deformable droplets⁹

$$U_{\text{sr}}(r, h) = \pi B_r \left(\frac{r^2 a^5}{h^7} + \frac{a^6}{6h^6} \right) \quad (8)$$

B_r is a parameter determining the magnitude of the repulsion. The short-range repulsion is most important in the film region. Numerical estimations show that the contribution of the surrounding spherical parts of the droplets (second term in eq 8) is often negligible.

The final contribution to the total interdroplet energy, U_s , is due to the extension of the interfaces, which inevitably accompanies the deformation (the droplets are incompressible). It reads^{4,19}

$$U_s(r) = \frac{\pi \gamma_0 r^4}{2a^2} \quad (9)$$

where γ_0 is the interfacial tension of the droplets before deformation. The Gibbs elasticity is ignored in the above expression, but it could be introduced as an additional term.^{4,19} In the case of microemulsions, for example, the interfacial tension becomes negligible and only the Gibbs elasticity term remains.⁴

The total energy then is

$$U(r, h) = U_{\text{vw}}(r, h) + U_{\text{el}}(r, h) + U_{\text{sr}}(r, h) + U_s(r) \quad (10)$$

Knowing the total energy is equivalent to knowing the equilibrium probability (see eq 3).

B. Diffusion Tensor. Expressions for the friction and diffusion tensor are derived in the Appendix. The general result for the diffusion tensor, $\mathbf{D}(r, h)$, we need is given by eqs A.10 through A.15. Below we will concentrate on the particular case of tangentially immobile droplet surfaces (see below), which leads to considerable simplifications, while being at the same time of significant practical importance. For this case we have (see the Appendix)

$$\mathbf{D} = kT \zeta^{-1} = \begin{pmatrix} D_{hh} & 0 \\ 0 & 0 \end{pmatrix} \quad (11)$$

where

$$D_{hh} = \frac{kT}{\zeta_{hh}} \quad (12)$$

This is the expression, used in the calculations below. ζ_{hh} (see eq A.10) is the hh -component of the hydrodynamic resistance tensor, ζ .

V. Numerical Results and Discussion for Droplets with Tangentially Immobile Surfaces

Droplets with tangentially immobile surfaces correspond to the case when the surfactants are soluble in the continuous phase and the droplet surfaces are saturated with adsorbed surfactant molecules. Now we can use eq 4 together with the results for $P_{\text{eq}}(r, h)$ and $\mathbf{D}(r, h)$ to find the mean escape time for the system from the secondary minimum. Note that using eq 11 for the diffusion tensor greatly simplifies eq 4 because

$$\mathbf{D}(r, h) \cdot \nabla \tau(r, h) = \begin{pmatrix} D_{hh} & 0 \\ 0 & 0 \end{pmatrix} \begin{pmatrix} \frac{\partial \tau}{\partial h} \\ \frac{\partial \tau}{\partial r} \end{pmatrix} = D_{hh}(r, h) \frac{\partial \tau}{\partial h} \mathbf{i}_h \quad (13)$$

Now eq 4 becomes

$$\frac{1}{P_{\text{eq}}(r, h)} \frac{d}{dh} \left[P_{\text{eq}}(r, h) D_{hh}(r, h) \frac{d\tau(r, h)}{dh} \right] = -1 \quad (14)$$

This is actually an ordinary differential equation and can be solved by direct integration. Hence

$$\tau(r, h, h^*) = \int_{h^*}^h \frac{dz}{P_{\text{eq}}(r, z) D_{hh}(r, z)} \int_z^{\infty} dy P_{\text{eq}}(r, y) \quad (15)$$

Equation 15 is the main result of the present study. The thickness h^* corresponds to the saddle point between the two minima. It may seem surprising that the result for the escape time does not depend explicitly on the viscosity of the droplet interior. This is due to the fact that the droplet surfaces are considered to be saturated with adsorbed surfactant molecules and therefore tangentially immobile.^{24,25} A more general situation (i.e. including tangential mobility of the droplet surfaces) will require consideration of the droplet viscosity, which is actually taken into account by the parameter ϵ^s (see the Appendix). Still, it was shown^{24,25} that for immiscible liquids of comparable viscosity and surfactants, soluble in the disperse media only, the contribution of the internal droplet flow on the film thinning is negligible.

The time $\tau(r, h, h^*)$, defined by eq 15 is the one needed for the system to cross the boundary $h = h^*$, starting from position with coordinates r and h . A very important feature of eq 14 is that its solution (eq 15) depends on the radial coordinate, although there are no derivatives with respect to r . This is due to the fact that both the equilibrium probability, $P_{\text{eq}}(r, h)$, and the diffusion coefficient, $D_{hh}(r, h)$, depend on the film radius.

Using the approach, described above, we calculate the mean escape (life) time for a doublet in the secondary energy minimum. For charged droplets, the stability depends strongly on the electrolyte concentration.^{1,5,6,28} That is why below we follow the change of the doublet life times with the electrolyte concentration. Two different

(27) Arfken, G. B.; Weber, H. J. *Mathematical Methods for Physicists*, 4th ed.; Academic Press: New York, 1995.

(28) Poulin, P.; Nallet, F.; Cabane, B.; Bibette, J. *Phys. Rev. Lett.* **1996**, *77*, 3248.

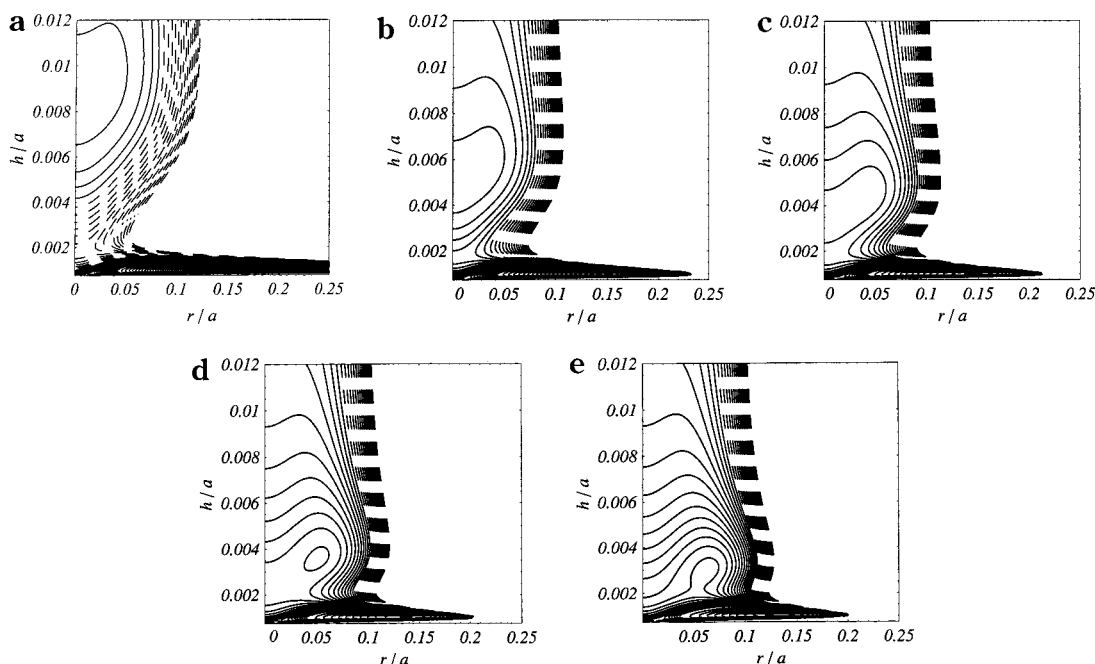


Figure 2. Case I. Contour diagram of the interaction energy for two droplets as a function of the film radius, r/a , and thickness, h/a . $A_H = 4 \times 10^{-21}$ J; surface potential, $\Psi_0 = 18$ mV; and droplet radius, $a = 500$ nm; and $\gamma = 4$ mN/m. (a) $C_{el} = 0.1$ M; (b) $C_{el} = 0.2$ M; (c) $C_{el} = 0.3$ M; (d) $C_{el} = 0.4$ M; (e) $C_{el} = 0.5$ M. The full contours correspond to negative energies; the dashed contours correspond to positive.

Table 1. Case I: Comparison of the Energy Minima, Saddle Point, and Escape Times for Droplets with and without Deformation (see Figure 2)^a

C_{el} , M	βU_m^d	βU_m^{nd}	βU_{sd}	τ^d , s	τ^{nd} , s
0.1	-6.78 $r/a = 0$ $h/a = 0.00837$	-6.78	12.98 $r/a = 0$ $h/a = 0.00178$	∞	∞
0.2	-11.12 $r/a = 0.01986$ $h/a = 0.00526$	-11.12	-3.29 $r/a = 0$ $h/a = 0.00168$	0.75	0.17
0.3	-15.41 $r/a = 0.03933$ $h/a = 0.00429$	-15.111	-12.96 $r/a = 0$ $h/a = 0.00173$	0.065	0.00059
0.4	-20.44 $r/a = 0.05190$ $h/a = 0.00359$	no minimum	-19.27 $r/a = 0$ $h/a = 0.00228$	0.0020	
0.5	-26.87 $r/a = 0.06254$ $h/a = 0.00298$	no minimum	-26.20 $r/a = 0.05392$ $h/a = 0.00225$	0.00028	

^a C_{el} is the electrolyte concentration. βU_m^d is the depth of the secondary energy minimum and βU_{sd} is the value of the energy at the saddle point in kT units. The respective values of the film thickness, h , and radius, r , are also given. τ^d and τ^{nd} are the mean escape times from the secondary minimum across the saddle point (barrier) for deformable and nondeformable droplets, respectively.

types of droplets are considered as examples. The first one (case I) is characterized by the Hamaker constant, $A_H = 4 \times 10^{-21}$ J; surface potential, $\Psi_0 = 18$ mV; droplet radius, $a = 500$ nm; and interfacial tension, $\gamma = 4$ mN/m, while the second (case II) is identical to the first but has a two times lower interfacial tension, $\gamma = 2$ mN/m. The repulsion parameter (see eq 8), was chosen to be $B_r = 6.25 \times 10^{-18} kT$. This values for the repulsion constant, B_r , was chosen by the only criterion that the film thickness in the primary minimum should be on the order of the hydrated (e.g., sodium) ion diameter, as is experimentally observed.²⁸ The temperature for all calculations was $T = 298$ K and the solvent viscosity $\eta = 0.89$ cP. Generally, the escape time, τ , is finite when transition from the secondary to the primary minimum is likely to occur and infinite when the energy barrier is too high. In the latter case the droplets may rebound.

The energy contour diagrams for case I are shown in Figure 2 and the respective escape times are in Table 1. The escape time for 0.1 M electrolyte concentration (Figure

2a) is infinite. This means that the system is trapped near the secondary minimum and the only option to leave it is go to state of infinite separation. Jumping into the primary minimum, however, is unlikely. Increasing the electrolyte concentration to 0.2 M (Figure 2b) has a dramatic effect on the escape time (see Table 1). It becomes $\tau = 0.75$ s. This is due to changes in the shape of the energy surface—the saddle point decreases from 12.98 kT (0.1 M) to -3.29 kT (0.2 M)—see Table 1. The droplets also deform in the secondary minimum for 0.2 M electrolyte, and comparison could be made with a referent hard sphere system. As shown in Table 1 the deformed spheres need almost four times longer time in order to escape from the secondary into the primary minimum, compared to hard spheres. This trend increases with further addition of electrolyte; for 0.3 M (Figure 2c), the deformed droplets escape time, τ , is more than 100 times greater than that for undeformed, τ_{nd} . Increasing the salt concentration to 0.4 M (Figure 2d) introduces a new substantial difference between the deformed and the referent undeformed droplets. There is

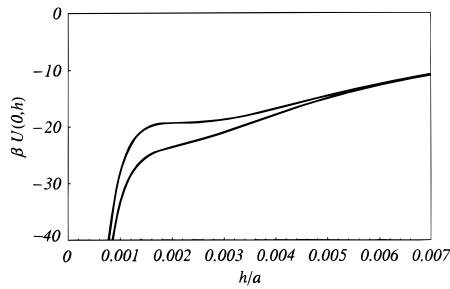


Figure 3. Interdroplet energy vs separation, h/a , at $r/a = 0$. The upper curve corresponds to parameters in Figure 2d ($C_{el} = 0.4$ M) and the lower to Figure 2e ($C_{el} = 0.5$ M).

a secondary energy minimum for the deformed droplets but not for the undeformed. This is shown clearly in Figure 3, which represents the energy vs separation curve for undeformed ($r = 0$) spherical droplets. Therefore, the transition into the primary minimum would have been barrierless if there was no deformation present. The escape time for the deformed droplets, τ , however, is finite although short. These features are even more pronounced for 0.5 M electrolyte (see Figures 2e and 3, and also Table 1). Again there is no secondary minimum in the energy curve for undeformed particles at this electrolyte concentration, and hence, the transition into the primary minimum is barrierless.

The effect of the droplet deformability on the doublet life time becomes much more important with further decreasing of the interfacial tension. Figure 4 and Table 2 present the results for case II, which is equivalent to case I except for the interfacial tension, which is two times less ($\gamma = 2$ mN/m instead of 4 mN/m). It is seen that there is virtually no difference between cases I and II at 0.1 M electrolyte concentration (cf. Figures 2a and 4a). This is because the electrostatic repulsion itself prevents the droplets from deformation at this electrolyte concentration. For $C_{el} = 0.2$ M, however, the escape time for deformed spheres increases significantly (see Figure 4b and Table 2) compared to the same electrolyte concentration but

greater interfacial tension ($\gamma = 4$ mN/m, Figure 2b and Table 1). There is a great difference also between the deformed and undeformed droplets. Increasing further the electrolyte concentration (Figure 4c–e) decreases the overall escape time, but the impact of the deformability (difference between deformed and undeformed droplets) on the escape time remains very substantial. Figure 5 shows the energy vs separation plot for undeformed spheres, and it is seen that there is no secondary minimum present, similarly to Figure 3.

There are systems where the interfacial tension could be even lower than 2 mN/m. A typical example is microemulsion forming oil/water/surfactant mixtures. In those cases the deformability effects are expected to be even stronger. Generally, the physical reasons for the greater doublet lifetime for deformable droplets are the following:

(1) The energy barrier for the deformed system is higher—the secondary minimum is deeper when film is formed.

(2) The hydrodynamic resistance is greater in the presence of plane parallel film.

(3) The distance, which the system has to travel from the secondary minimum to the saddle point, is longer when deformation is present.

Other possible factors that may affect the escape time are the curvatures in the secondary minimum, $a^2(\partial^2\beta U/\partial h^2)_{\min}$, and the saddle point, $a^2(\partial^2\beta U/\partial h^2)_{\text{saddle}}$. We did not find a well-defined correspondence with the variation of these curvatures and the respective escape times for the different cases; therefore, one may conclude that their impact, if any, is more subtle.

The secondary film lifetime is related to the rate constant in kinetic schemes, developed for ensembles of droplets; hence, it is important for the macroscopic behavior and stability of emulsions.^{5,13,14} If there are not sufficiently strong short-ranged repulsive forces the film in the primary minimum, it would not be stable and the droplets would coalesce. In this case the mean escape time is actually the coalescence time of two emulsion droplets.

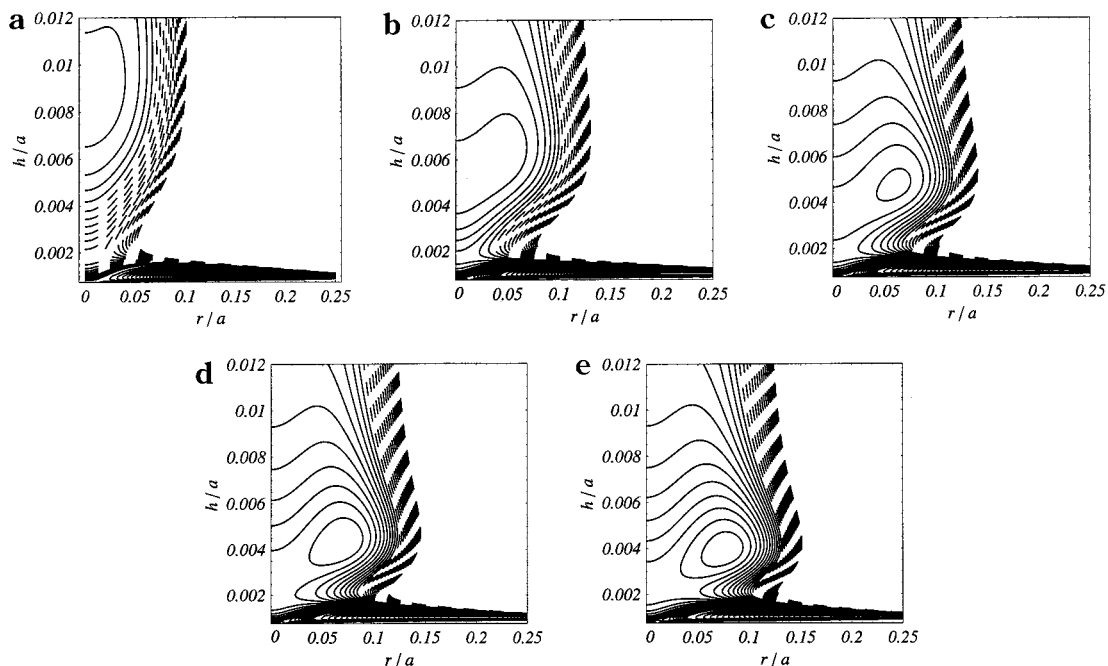


Figure 4. Case II. Contour diagram of the interaction energy for two droplets as a function of the film radius, r/a , and thickness. $A_H = 4 \times 10^{-21}$ J; surface potential, $\Psi_0 = 18$ mV; and droplet radius, $a = 500$ nm; and $\gamma = 2$ mN/m. (a) $C_{el} = 0.1$ M; (b) $C_{el} = 0.2$ M; (c) $C_{el} = 0.3$ M; (d) $C_{el} = 0.35$ M; (e) $C_{el} = 0.4$ M. The full contours correspond to negative energies; the dashed contours correspond to positive.

Table 2. Case II: Comparison of the Energy Minima, Saddle Point, and Escape Times for Droplets with and without Deformation (see Figure 4)^a

C_{el}, M	βU_m^d	βU_m^{nd}	βU_{sd}	$\tau_{0.25}^d, s$	$\tau_{0.25}^{nd}, s$
0.1	-6.78	-6.78	12.98	∞	∞
	$r/a = 0$ $h/a = 0.00837$	$h/a = 0.00837$	$r/a = 0$ $h/a = 0.00178$		
0.2	-11.33	-11.12	-3.29	636.36	0.17
	$r/a = 0.04236$ $h/a = 0.00594$	$h/a = 0.00492$	$r/a = 0$ $h/a = 0.00168$		
0.3	-16.59	-15.11	-12.96	243.29	0.00059
	$r/a = 0.06130$ $h/a = 0.00475$	$h/a = 0.00339$	$r/a = 0$ $h/a = 0.00173$		
0.35	-19.81	-17.12	-16.49	63.91	0.000 12
	$r/a = 0.06919$ $h/a = 0.00430$	$h/a = 0.00282$	$r/a = 0$ $h/a = 0.00182$		
0.4	-23.55	no minimum	-26.20	0.00028	
	$r/a = 0.07662$ $h/a = 0.00392$		$r/a = 0.01518$ $h/a = 0.00221$		

^a All quantities are the same as in Table 1.

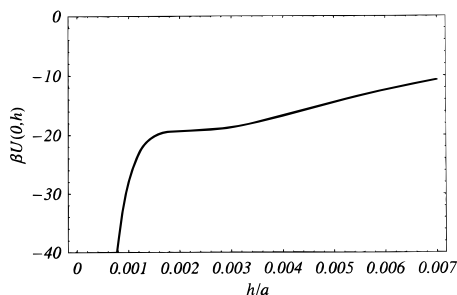


Figure 5. Interdroplet energy vs separation, h/a , at $r/a = 0$. The upper curve corresponds to parameters in Figure 4e ($C_{el} = 0.4 M$).

The model, suggested in this study, does not account for wavelike disturbances of the film surfaces. As mentioned above, the main reason for that is the experimental evidence available, showing that upon decreasing the film radius, its surfaces become less prone to corrugations and wavelike deformations;¹² see also ref 29. Direct observation showed that film thinning of large films is accompanied with thickness fluctuations and dimpling of the surfaces, while in the case of smaller ones (micron sized) such phenomena are not present.¹² Thinning rate experiments also revealed that small films thin according to the Reynolds formula,²⁹ which was derived for the case of two approaching parallel solid disks in viscous fluid. In other words, the film surfaces do not exhibit any corrugations according to this experiment. Theoretical estimates³⁰ also imply that wavelike fluctuations are unlikely for film radii on the order of those considered in the present paper. Finally, it was shown³¹ that experimental results for osmotic-compression-induced coalescence in miniemulsions could be explained in the framework of simple DLVO model without involving the squeezing mode thickness fluctuations. Simply by applying osmotic stress the film is forced to pass over the electrostatic force barrier, which stabilizes the droplets.

There is no restriction for other types of colloidal interactions to be involved in the approach, described here. The present study deals mainly with DLVO interactions, but others like hydration, hydrophobic, and steric could be treated in a similar way. Particularly interesting is the case of larger droplets interacting in the presence of smaller ones. For example, these could be emulsion drops

in the presence of microemulsion droplets. In this case the energy surface could have a complex shape with multiple minima.⁹ Hence, one may also expect to have multiple escape times, and since the minima might be of comparable depth, the transitions may take place backwards as well as forwards. The main theoretical difficulty for such systems is the calculation of the diffusion (friction) tensor, because it requires knowledge about the flow of concentrated dispersion (e.g., microemulsion) in confined spaces (thin film between the large emulsion drops).

VI. Conclusions

The balance between attractive and repulsive interaction may lead to the formation of doublets of deformed droplets even when they are in the submicron range.^{4,7-9} The importance of this deformation (film formation) on the lifetime of the aggregates is usually ignored or explicitly considered unimportant.^{13,14} The present study shows that this is not always correct. Emulsion systems with low interfacial tension and/or at high electrolyte concentration are in general affected by the deformation. The film formed within such a droplet doublet is represented as a virtual Brownian particle, undergoing random motion in the two-dimensional space of the film radius, r , and thickness, h . This notion allows us to apply stochastic analysis (in terms of the Smoluchowski equation for the evolution of the probability function) to calculate the secondary doublet lifetime (escape time from the secondary into the primary energy minimum). It increases with the appearance of the plane parallel film with finite radius if compared to that for referent hard spheres. The droplet deformation actually changes the whole shape of the energy surface and is usually accompanied by greater film thickness and deeper secondary energy minima (see Tables 1 and 2). This leads to different pathways for the thickness transitions for deformable and undeformable droplets.

Acknowledgment. I am indebted to Drs. P. Vekilov and J. Satulovsky for reading the first draft of the manuscript and making some useful comments. This study was supported by grants from NASA (NAG8-1354) and National Institute of Health (NIH R01 HL58038).

VII. Appendix: Calculation of the Friction and Diffusion Tensors

In this Appendix we calculate the components of the friction tensor, $\zeta(r, h)$, which is needed to obtain the

(29) Radoev, B.; Scheludko, A.; Manev, E. *J. Colloid Interface Sci.* **1983**, *95*, 254.

(30) Tsekov, R. *Colloids Surf.* **1998**, *141*, 161.

(31) Petsev, D. N.; Bibette, J. *Langmuir* **1995**, *11*, 1075.

diffusion tensor, $\mathbf{D}(r,h)$. Both are related by the equation

$$\mathbf{D}(r,h) = kT\zeta^{-1}(r,h) \quad (\text{A.1})$$

The friction tensor components could be easily derived using results from ref 4 and elements of the nonequilibrium thermodynamics, i.e., Onsager reciprocal relations.²² It is assumed that the droplets shape is always that of truncated spheres. For linear flows we can write

$$\mathbf{F} = \zeta \cdot \mathbf{V} \quad (\text{A.2})$$

or in terms of components

$$F_h = \zeta_{hh}V_h + \zeta_{hr}V_r \quad (\text{A.3})$$

$$F_r = \zeta_{rh}V_h + \zeta_{rr}V_r$$

Onsager theorem²² claims that $\zeta_{hr} = \zeta_{rh}$. Now we can make use of the particular case, $F_r = 0$; i.e., no radial force is applied. This case was analyzed in ref 4. Equation A.3 transforms into

$$F_h = \zeta_{hh}V_h + \zeta_{hr}V_r \quad (\text{A.4})$$

$$0 = \zeta_{hr}V_h + \zeta_{rr}V_r$$

On the other hand, it was shown^{4,24} that the force normal to the film surfaces is

$$F_h = -\pi \int_0^\infty dx x^2 \left(\frac{\partial P_s}{\partial x} \right) \quad (\text{A.5})$$

The integration is performed radially in the plane of one of the film surfaces with x being the running radial coordinate. P_s is the radial distribution of the scalar pressure at the droplet surfaces. Lubrication theory gives²⁴

$$\frac{\partial P_s}{\partial x} = -\frac{6\eta x}{H^3}V_h + \frac{12\eta}{H^2}V_x(x) \quad (\text{A.6})$$

where for small separations

$$H = h \quad \text{for } x \leq r \quad (\text{A.7})$$

$$H = h - \frac{r^2}{a} + \frac{x^2}{a} \quad \text{for } x > r$$

The radial velocity $V_x(x)$ is a linear function of the running radial coordinate x^4

$$V_x(x) = \frac{V_r x(1 - \epsilon^s)}{2H} \quad (\text{A.8})$$

The parameter ϵ^s is related to the tangential mobility of the droplet surfaces as well as to the viscous properties of the droplets;^{24,25} see also ref 4. $\epsilon^s = 1$ corresponds to tangentially immobile surfaces, and in this case the droplet viscosity does not play a role. For mobile interfaces $\epsilon^s < 1$. The radial velocity could be expressed as

$$V_x(x) = \frac{x}{r}V_r \quad (\text{A.9})$$

where $V_r = V_x(r)$ is the value at the film periphery (cf. eq A.4). Combining A.5 through A.9 we obtain

$$\begin{aligned} \zeta_{hh} &= 6\pi\eta \left[\int_0^r dx \frac{x^3}{h^3} + \int_r^\infty dx \frac{x^3}{\left(h - \frac{r^2}{a} + \frac{x^2}{a}\right)^3} \right] \quad (\text{A.10}) \\ &= \frac{3\pi\eta a^2}{2h} \left(1 + \frac{r^2}{ah} + \frac{r^4}{a^2 h^2} \right) \end{aligned}$$

and

$$\begin{aligned} \zeta_{hr} &= \zeta_{rh} \quad (\text{A.11}) \\ &= -\frac{12\pi\eta}{r h^2} \int_0^r dx x^3 = -\frac{3\pi\eta r^3}{h^2} \end{aligned}$$

Taking the second equation (A.4) and using⁴

$$\frac{V_h}{V_r} = \frac{2h}{r(1 - \epsilon^s)} \quad (\text{A.12})$$

one can calculate the radial component of the friction tensor

$$\begin{aligned} \zeta_{rr} &= \frac{24\pi\eta}{r^2 h(1 - \epsilon^s)} \int_0^r dx x^3 \quad (\text{A.13}) \\ &= \frac{6\pi\eta r^2}{h(1 - \epsilon^s)} \end{aligned}$$

For the derivation of the diffusion tensor we need to calculate ζ^{-1} , which is²⁷

$$\zeta^{-1} = \frac{1}{\det(\zeta)} \begin{pmatrix} \zeta_{rr} & -\zeta_{hr} \\ -\zeta_{hr} & \zeta_{hh} \end{pmatrix} = \frac{1}{\zeta_{hh}\zeta_{rr} - \zeta_{hr}^2} \begin{pmatrix} \zeta_{rr} & -\zeta_{hr} \\ -\zeta_{hr} & \zeta_{hh} \end{pmatrix} \quad (\text{A.14})$$

Hence, the components of the diffusion tensor are (see eq A.1)

$$D_{hh} = \frac{kT\zeta_{rr}}{\zeta_{hh}\zeta_{rr} - \zeta_{hr}^2} = \frac{kT}{\zeta_{hh} \left(1 - \frac{\zeta_{hr}^2}{\zeta_{hh}\zeta_{rr}} \right)}$$

$$D_{hr} = D_{rh} = \frac{-kT\zeta_{hr}}{\zeta_{hh}\zeta_{rr} - \zeta_{hr}^2} = \frac{-kT}{\frac{\zeta_{hh}\zeta_{rr}}{\zeta_{hr}} \left(1 - \frac{\zeta_{hr}^2}{\zeta_{hh}\zeta_{rr}} \right)} \quad (\text{A.15})$$

$$D_{rr} = \frac{kT\zeta_{hh}}{\zeta_{hh}\zeta_{rr} - \zeta_{hr}^2} = \frac{kT}{\zeta_{rr} \left(1 - \frac{\zeta_{hr}^2}{\zeta_{hh}\zeta_{rr}} \right)}$$

An important case is that of droplets with tangentially immobile surfaces where $\epsilon^s = 1$ and $\zeta_{rr} \rightarrow \infty$. Then one obtains

$$D_{hh} = \frac{kT}{\zeta_{hh}} \quad (\text{A.16})$$

$$D_{hr} = D_{rh} = D_{rr} = 0$$

or

$$\mathbf{D} = \begin{pmatrix} D_{hh} & 0 \\ 0 & 0 \end{pmatrix} \quad (\text{A.17})$$